International Journal of Mechanical, Industrial and Aerospace Sciences
ISSN: 2517-9950
Vol:9, No:6, 2015

Investigation of Bubble Growth during Nucleate Boiling Using CFD

K. Jagannath, Akhilesh Kotian, S. S. Sharma, Achutha Kini U., P. R. Prabhu

***Abstract*—**Boiling process is characterized by the rapid formation of vapour bubbles at the solid–liquid interface (nucleate boiling) with pre-existing vapour or gas pockets. Computational fluid dynamics (CFD) is an important tool to study bubble dynamics. In the present study, CFD simulation has been carried out to determine the bubble detachment diameter and its terminal velocity. Volume of fluid method is used to model the bubble and the surrounding by solving single set of momentum equations and tracking the volume fraction of each of the fluids throughout the domain. In the simulation, bubble is generated by allowing water-vapour to enter a cylinder filled with liquid water through an inlet at the bottom. After the bubble is fully formed, the bubble detaches from the surface and rises up during which the bubble accelerates due to the net balance between buoyancy force and viscous drag. Finally when these forces exactly balance each other, it attains a constant terminal velocity. The bubble detachment diameter and the terminal velocity of the bubble are captured by the monitor function provided in FLUENT. The detachment diameter and the terminal velocity obtained are compared with the established results based on the shape of the bubble. A good agreement is obtained between the results obtained from simulation and the equations in comparison with the established results.

***Keywords*—**Bubble growth, computational fluid dynamics, detachment diameter, terminal velocity.

I. Introduction

A. Bubble Growth and Detachment Diameter

ONCE the vapour bubble on the heater surface is large enough at a given temperature that nucleation is assured, it will begin to grow in size. With the increase in temperature difference with the associated pressure difference causes the bubble to grow. The prime forces acting on a vapour bubble during the later phases of its growth are buoyancy and hydrodynamic drag forces attempting to detach it from the surface and surface tension and liquid inertia forces acting to prevent detachment. The liquid inertia force is a dynamic force resulting from the displacement of bubble during bubble growth. The growth velocity of a bubble and hence the initial force is a strong function of the liquid superheat which, in turn, is inversely proportional to the size of the active cavity. A small cavity thus forms a bubble with a faster growth rate than from a large cavity. Fritz and Ende [1] have considered all the forces acting on a growing bubble and have concluded that for small cavity sizes ($r_c < 10$ μm for water at atmospheric pressure) the bubble size at departure is dictated mainly by balance between buoyancy and liquid inertia forces. For larger cavity sizes, the growth rate decreases, the dynamic forces become small, and the bubble size at departure is set by a balance between buoyancy and surface tension forces. Fritz and Ende [1] first considered this case and proposed the following equation for the detachment diameter:

$$D_d = 0.0208\theta \left[\frac{\sigma}{g(\rho_l - \rho_g)}\right]^{\frac{1}{2}} \quad (1)$$

Bozzano and Dente [2] presented a new approach by a unified model for the description of single bubble motions. They gave equations to determine the terminal velocity and also to determine the shape of the bubble. They studied the effects of diameter of the domain in which the bubble rises. Predictions were compared against experimental data for a wide range of physical properties and size of bubbles

Amaya-Bower and Lee [3] studied the dynamics of a single rising gas bubble using Lattice Boltzmann Method (LBM). They studied the factors on which the deformation of bubbles takes place. They deduced that the velocity of the bubble depends on the balance of other forces produced by surface tension, inertia, and viscosity. Clift et al [4] developed a numerical method to simulate the compressible bubble dynamics. VOF approach was used to capture the interface effects of the bubble.

B. Terminal Velocity of the Bubble

Terminal velocity is defined as the steady velocity that the bubble reaches when there is a balance between buoyancy and drag forces. The relative terminal rising velocity of a single gas bubble, moving into a liquid phase, is determined by its size, by the interfacial tension and by the density and viscosity of the surrounding liquid. Both shape and velocity are strongly interacting. Bozzano and Dente [2] have obtained equations to determine the terminal rising velocity of a single bubble. They have represented the bubble shape by means of the superposition of two oblate semi-spheroids (Fig. 1) having a common larger semi-axis. Asymptotically, the shape can degenerate towards something resembling a spherical-cap or towards a spherical bubble. Validity of the proposed expression is restricted to Morton Numbers less than 1E-8. Hua and Lou [5] used an improved numerical algorithm which uses volume correction to conserve the bubble volume while tracking the bubble rise and deformation of a rising bubble in a quiescent viscous liquid. This method is validated by

Jagannath K, Professor, Akhilesh Kotian, P.G student, S. S. Sharma, Professor, and Achutha Kini U, Professor, are with the Department of Mechanical & Manufacturing Engineering, Manipal Institute of Technology, Manipal - 576104 (e-mail: jagan.korody@manipal.edu, akhilkotian_6@yahoo.co.in, ss.sharma@manipal.edu, achutha.kini@manipal.edu).

P. R. Prabhu, Associate Professor, Department of Mechanical Manufacturing Engineering, Manipal Institute of Technology, Manipal - 576104 (Phone: 0820 2925463; Fax: 0820 2571071; e-mail: raghu.prabhu@manipal.edu).

simulating single bubble rising and deforming in quiescent viscous liquid under different flow regimes and is compared with the experimental data on terminal bubble shape and velocity. Chetal et al [7] described the design of prototype fast breeder reactor including reactor core, reactor assembly, heat transport system etc. Filip Gottfridsson [8] examined the various causes for core-flowering in fast breeder reactor by simulation to find out negative reactor transients.

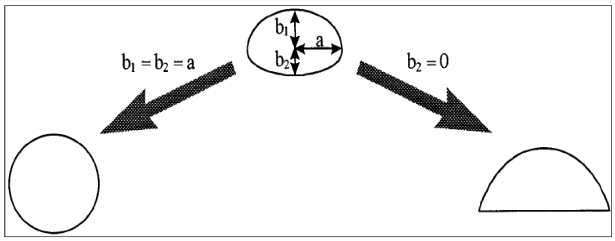

Fig. 1 Basic shape of the bubble and asymptotic degeneration [2]

The bubble motion is assumed linear and secondary motions (i.e. helicoildal, zigzag, oscillating) are neglected. When steady state motion has been reached, the forces balanced around the bubble gives

$$(\rho_L - \rho_g) g V_B = \pi a^2 \frac{\rho_l U_o^2}{2} f \quad (2)$$

By neglecting the gas density in comparison with that of the liquid, above equation gives the terminal rising velocity in infinite environment

$$U_0^2 = \frac{4}{3}\frac{gD_0}{C_D} \quad (3)$$

where

$$C_D = f\left(\frac{a}{R_0}\right)^2 \quad (4)$$

The proposed generalized friction factor (f) is such to cover a wide range of Reynolds, Eotvos and Morton numbers [2].

$$f = \frac{48}{Re}\left(\frac{1+12Mo^{1/3}}{1+36Mo^{1/3}}\right) + 0.9\left[\frac{Eo^{3/2}}{1.4(1+30Mo^{1/6})}\right] \quad (5)$$

The interpolation of the numerical results obtained through the minimization procedure can give a first approximation expression of the deformation factor (DEF), resulting in

$$DEF = \left(\frac{a}{R_0}\right)^2 \cong \frac{2}{x+y} \cong \frac{10\left(1+1.3Mo^{\frac{1}{6}}\right)+3.1Eo}{10\left(1+1.3Mo^{\frac{1}{6}}\right)+Eo} \quad (6)$$

The drag co-efficient can be then estimated by the product of (5) and (6) and therefore it becomes an approximate explicit function of Eo, Mo and Re numbers. Finally by substituting (4) into (3) a simple second order equation is generated, that gives place to U_0. Terminal velocity also depends on the final shape of the bubble.

The correlation for three regimes i.e. spherical, ellipsoidal and spherical has been provided as:

Spherical Regime:

In this regime, the terminal velocity is proportional to size of the bubble. The terminal rising velocity has been described for this regime as:

$$U_0 = \frac{gD_0^2\Delta\rho}{6\mu_l}\frac{(1+k_1)}{(2+3k_1)} \quad (7)$$

Ellipsoidal Regime:

In this regime, there is little viscous resistance to internal circulation, therefore drag and terminal velocity is very sensitive to contamination. Terminal velocity for pure systems is closely approximated by a correlation based on wave theory as:

$$U_0 = \sqrt{\frac{2.14\,\sigma}{\rho_l D_o} + 0.505 g D_o} \quad (8)$$

Spherical Cap Regime:

This regime is governed by inertia force. In this regime, terminal velocity of bubble is proportional to size. In addition, large inertia creates higher deformation by creating high pressure on the front and rear and while low at the sides. Rising velocity has been described as:

$$U_0 = \frac{2}{3}\sqrt{\frac{gD_0\Delta\rho}{2\rho_l}} \quad (9)$$

II. Methodology

For all flow related problems, conservation equations for mass and momentum has to be solved. For flows involving heat transfer or compressibility, an additional equation for energy conservation is solved. For flows involving species mixing or reactions, a species conservation equation is solved or, if the non-premixed combustion model is used, conservation equations for the mixture fraction and its variance are solved. Additional transport equations are also solved when the flow is turbulent.

In the present work we will be dealing with laminar models with no compressibility effects and laminar models with compressibility effects.

A. Laminar Models without Compressibility Effects

All the problems in the present work are carried out using laminar models. Hence equations for turbulence are not considered. When the density of the phases is fixed, the problem becomes an incompressible problem. Hence, energy equation is not solved in this case.

1. Mass Conservation Equation:

The equation for conservation of mass, or continuity equation, can be written as

$$\frac{\partial \rho}{\partial t} + \nabla.(\rho \vec{v}) = S_m \quad (10)$$

The source S_m is the mass added to the continuous phase from the dispersed second phase (e.g., due to vaporization of liquid droplets) and any user-defined sources.

2. Momentum Conservation Equation:

The equation for Conservation of momentum, or momentum equation, can be written as [4]:

$$\frac{\partial(\rho\vec{v})}{\partial t} + \nabla.(\vec{v}\vec{v}) = -\nabla.p + \nabla.[\mu(\nabla\vec{v})] + \rho\vec{g} + \vec{F} \quad (11)$$

where p is the static pressure, $\mu(\nabla\vec{v})$ is the stress tensor term, μ is the viscosity and $\rho\overrightarrow{g}$ and $\overrightarrow{F}$ are the gravitational body force and external body forces (e.g., centrifugal force), respectively.

3. Volume Fraction Equation:

The tracking of the interface(s) between the phases is accomplished by the solution of a continuity equation for the volume fraction of one (or more) of the phases. For the qth phase, this equation has the following form [4]:

$$\frac{1}{\rho_q}\left[\frac{\partial}{\partial t}(\alpha_q\rho_q) + \nabla.(\alpha_q\rho_q\vec{v}_q) = S_{\alpha_q} + \sum_{p=1}^{n}(\dot{m}_{pq} - \dot{m}_{qp})\right] \quad (12)$$

where $\dot{m}_{qp}$ *is* the mass which is transferred from phase q to phase p and $\dot{m}_{pq}$ is the mass transfer from phase p to phase q. By default, the source term on the right-hand side of (12), S_{α_q}, is zero, but one can specify a constant or user-defined mass source for each phase.

The volume fraction equation will not be solved for the primary phase; the primary-phase volume fraction will be computed based on the following constraint:

$$\sum_{q=1}^{n}\alpha_q = 1 \quad (13)$$

The VOF model can also include the effects of surface tension along the interface between each pair of phases. The addition of surface tension to the VOF calculation results in a source term in the momentum equation.

III. Description of the Problem

Consider a cylinder of certain radius filled with water which is open to atmosphere. A small inlet is provided at the bottom of the cylinder through which water-vapor is injected at a constant mass flow rate. The jet rises inside the cylinder forming a vertical column due to the jet effects and the momentum of the incoming fluid. At some time, the buoyancy force overcomes the restraining effects of the surface tension attaching the bubble to the surface. Thereafter, the bubble detaches from the surface and rises up. Once the bubble has detached from the surface, injection of vapor into the cylinder is stopped in order to capture the effects of only one bubble. Because of the surface tension, initially the bubble tends to a circular shape. During its upward motion, the bubble will be accelerated due to the net balance between buoyancy force and viscous drag. Finally when these forces exactly balance each other, it attains a constant terminal velocity. The terminal velocity of the bubble is captured by the monitor function provided in FLUENT [6].

A. Modeling and Meshing Details

The above mentioned phenomenon is modelled by using a 2-D axi-symmetric slab model of a cylindrical container of radius 5 mm and height 60 mm as shown in Fig. 2. The model is meshed with simple hexahedral meshes as shown in Fig. 3.

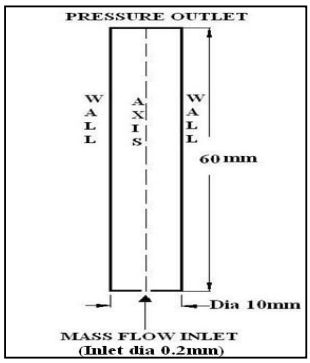

Fig. 2 Schematic diagram of model

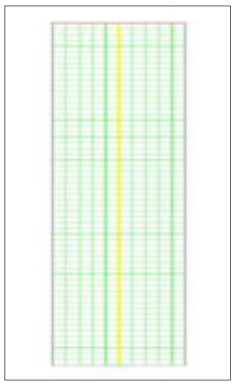

Fig. 3 Computational grid

B. Boundary Conditions

The inlet mass flow rate of water vapour is 1e-7 kg/s. The walls of the cylinder are assigned the wall boundary condition with 'slip' condition. Pressure outlet is provided at the top. Gravity acceleration is taken equal to g = 9.81 m/s^2, the surface tension is 0.05833 N/m and the angle of contact between water and water vapour is 90 °.

TABLE I
PHYSICAL PARAMETERS OF VAPOUR AND WATER

Fluid	Density (kg/m^3)	C_p (J/kg-K)	Thermal conductivity (W/m-K)	Viscosity (kg/m-s)
Water- liquid	998.2	4182	0.6	0.001003
Water- vapour	0.5542	2014	0.0261	1.34E-05

C. Material Properties

In this problem two fluids are considered, namely water-vapour (light fluid) and water (heavy fluid).The physical

parameters of the injected fluid i.e., vapour and the surrounding water is given in Table I.

TABLE II
RESULTS OF MESH INDEPENDENCE STUDY FOR BUBBLE DETACHMENT DIAMETER

Case	Grid Size	Bubble detachment Diameter, D_d (mm)
A1	0.20mm x 0.20mm	5.11
A2	0.15mm x 0.15mm	5.31
A3	0.10mm x 0.10mm	5.41
Theoretical (from (1))		*4.59*

D.Solver Details

A pressure based solver, 1st order implicit unsteady formulation and Green-Gauss cell based gradient option is used. Unsteady process is adopted here to acquire the shape of the bubble in different time step. Pressure and pressure velocity coupling discretization are Presto and SIMPLE scheme, respectively. Other discretization adopts First order upwind for density, energy and momentum. A first order accurate in space and time computation is performed using a fixed time step, Δt = 1e-05 s. Initially, before the air is injected, a small hemispherical bubble of 0.4 mm is created at the inlet in order to avoid a sharp discontinuity in the surface tension.

E. Mesh Independence Study

The simple problem geometry allows for efficient discretization of the domain using plane quadrilateral cells. Different grid sizes were examined to investigate the sensitivity and the accuracy of the results. Table II shows the results for bubble departure diameter obtained for three different mesh sizes. The bubble detachment diameter is determined for each case. The results are also compared with the theoretical results obtained with (1).

IV. RESULTS AND DISCUSSION

The sequence of bubble formation, departure and the change in bubble shapes during the rise of the bubble in the container at different time intervals is shown in Fig. 4.

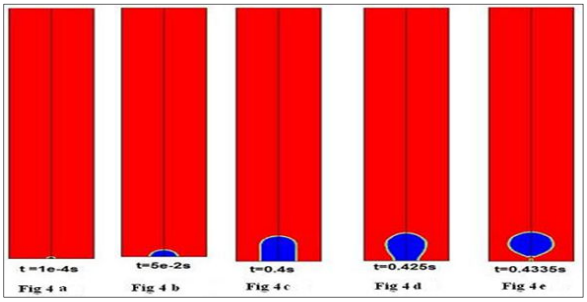

Fig. 4 Sequence of bubble detachment

After the bubble has detached from the surface, the flow of vapour is stopped. The bubble is allowed to rise in the quiescent fluid. The sequence of bubble rise in the cylinder at different time intervals is shown in Fig. 5.

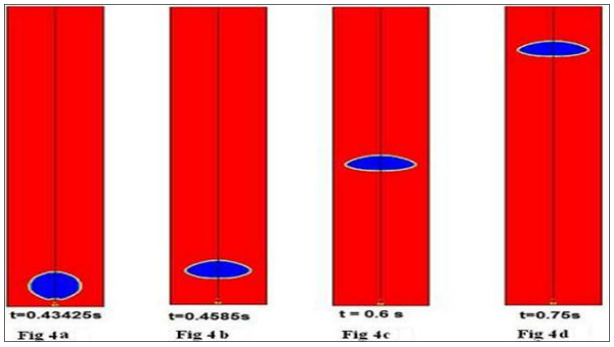

Fig. 5 Sequence of bubble rise

As the jet rises inside the cylinder, a vertical column formed is shown in Fig. 4 (c). Fig. 4 (d) shows the process of bubble slowly detaching from the surface. Finally the bubble detaching from the surface completely is shown in Fig. 4 (e). After the detachment, the bubble initially tends to a circular shape due to surface tension as shown in Fig. 5 (a).

The bubble rising velocity is plotted against time as shown in Fig 6. It is seen that after initial oscillations, the bubble stabilizes and reaches a constant terminal velocity.

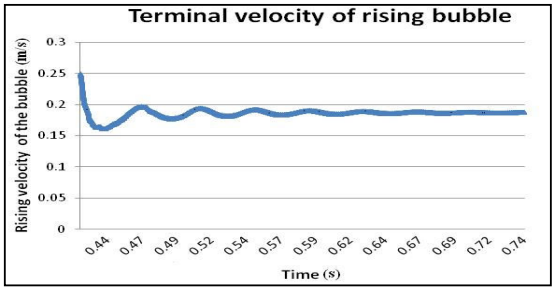

Fig. 6 Velocity of rising bubble versus time

The results obtained from simulation are compared with the theoretical results in Table III.

TABLE III
COMPARISON BETWEEN SIMULATION AND THEORETICAL TERMINAL VELOCITY

Cases	Terminal velocity (m/s)
Present simulation	0.190
G.Bozzano, M. Dente [2] (solving (3))	0.219
Clift R, Grace JR, Weber M [3], (solving (8))	0.223

V. CONCLUSION

1) As the mesh size decreases, the size of the bubble increases, however the value of the detachment converges.
2) Once the bubble has detached from the surface, the velocity of the rising bubble is oscillating in the beginning. This is because the fluid inside the bubble keeps rotating. After some time, the bubble stabilizes and attains terminal velocity.

3) The bubble detachment diameter agrees well with theoretical equations and the small difference in the values between the theoretical and simulation result is because the equation 1 available for detachment diameter is for small cavity sizes. However, further decreasing the inlet diameter in the simulation model will lead to convergence issues.
4) The values obtained for terminal velocity matches with the theoretical results.

NOMENCLATURE

ρ Density
t Time
$\vec{v}$ Velocity vector
r_c Radius of cavity
D_d Departure diameter
θ Angle of contact
σ Surface tension
g Acceleration due to gravity
p Local relative (or gauge) pressure
p_{op} Operating pressure
M_w Molecular weight of the gas
ρ_l Density of liquid
ρ_g Density of gas
V_B Volume of the bubble
a bubble major semi-axis
b1, b2 bubble minor semi-axes
U_0 Terminal velocity of the rising bubble
f Friction factor
D_0 Initial diameter of the bubble
R_0 Initial radius of the bubble
C_D Drag co-efficient
μ_l Absolute viscosity of the liquid
μ_g Absolute viscosity of the gas
Re Reynolds number $= \frac{\rho_l D_0 U_0}{\mu_l}$
E_0 Eotvos number $= \frac{(\rho_l - \rho_g) g D_0^2}{\sigma}$
Mo Morton number $= \frac{g \mu_l^4}{\rho_l \sigma^3}$
Bo Bond number $= \frac{(\rho_l - \rho_g) g D_0^2}{\sigma}$
k_1 Viscosity ratio $= \frac{\mu_l}{\mu_g}$

REFERENCES

[1] John G Collier, "Convective Boiling and Condensation", Second edition, McGraw Hill International Book Company, 1981.
[2] G. Bozzano, M. Dente, "Shape and terminal velocity of single bubble motion: a novel approach", Computers and chemical engineering, 2001, 25, 571-576.
[3] Luz Amaya-Bower, Taehun Lee, "Single bubble rising dynamics for moderate Reynolds number using Lattice Boltzmann Method", Computers & Fluids (2010), 39, 1191–1207.
[4] Clift R, Grace JR, Weber M. "Bubbles, drops, and particles", New York, Academic Press, 1978.
[5] Hua J, Stene JF, Lin P, "Numerical simulation of 3D bubble rising in viscous liquids using a front tracking method", J Comput Phys 2008, 227, 3358–82.
[6] Fluent 6.3, user's guide, Fluent. Inc Canonsburg, 2006.
[7] S.C. Chetal et al, "The design of the prototype fast breeder reactor", Nuclear engineering and design, 2006, 236, 852-860.
[8] Filip Gottfridsson, "Simulation of Reactor Transient and Design Criteria of Sodium cooled Fast Reactors", Uppsala university, France, 2011.

Jagannath K. holds Bachelor's degree in Mechanical Engineering (Bangalore University, India 1983), Master's degree in Engineering Management (Mangalore University, India 1990) and PhD degree in Tribology (MAHE University, India 2007). He has 30 years of teaching experience. His area of interest includes Tribology, Refrigeration and air conditioning, Renewable energy systems. He has published 30 research papers in journals and presented 40 research papers in conferences.

S. S. Sharma holds Bachelor's degree in Industrial & Production Engineering (Mysore University, India 1987), Master's degree in Materials Engineering (Mangalore University, India 1996) and PhD degree in Materials Engineering (Manipal University, India 2007). He has 24 years of teaching experience. His area of interest includes Heat Treatment, Deformation of Metals, Material Characterization, Composite Materials. He has published 28 research papers in journals and presented 47 research papers in conferences.

Achutha Kini U holds Bachelor's degree in Mechanical Engineering (Mysore University, India 1985), Master's degree in Engineering Management (Mangalore University, India 1991) and PhD degree in Corrosion Engineering (Manipal University, India 2012). He has 24 years of teaching experience. His area of interest includes Corrosion Science and Engineering, Composite Materials. He has published 18 research papers in journals and presented 32 research papers in conferences.

P. R. Prabhu received his Bachelor's Degree in Mechanical Engineering (Mangalore University, India 2001) and Master's Degree in Engineering Management (MAHE University, India 2003) and PhD degree in manufacturing (MAHE University, India 2003). His area of interest includes Manufacturing, Metallurgy, Design of Experiments for Mechanical Engineering Problems. He has published 15 research papers in journals and presented 30 research papers in conferences.